Received: 29 July 2020 | Revised: 9 October 2020 | Accepted: 1 November 2020

DOI: 10.1002/jms.4679



RESEARCH ARTICLE

Journal of MASS SPECTROMETRY WILEY

# Comparison of in-source collision-induced dissociation and beam-type collision-induced dissociation of emerging synthetic drugs using a high-resolution quadrupole time-of-flight mass spectrometer

J. Tyler Davidson[1,3] | Zachary J. Sasiene[2] | Glen P. Jackson[1,2]

[1]Department of Forensic and Investigative Science, West Virginia University, Morgantown, West Virginia, USA

[2]C. Eugene Bennett Department of Chemistry, West Virginia University, Morgantown, West Virginia, USA

[3]Department of Forensic Science, Sam Houston State University, Huntsville, Texas, USA

**Correspondence**
Glen P. Jackson, Department of Forensic and Investigative Science, West Virginia University, Morgantown, WV 26506-6121, USA.
Email: glen.jackson@mail.wvu.edu

**Funding information**
National Institute of Justice, Office of Justice Programs, and U.S. Department of Justice, Grant/Award Number: 2018-75-CX-0033

## Abstract

In-source collision-induced dissociation (CID) is commonly used with single-stage high-resolution mass spectrometers to gather both a molecular formula and structural information through the collisional activation of analytes with residual background gas in the source region of the mass spectrometer. However, unlike tandem mass spectrometry, in-source CID does not involve an isolation step prior to collisional activation leading to a product ion spectrum composed of fragment ions from any analyte present during the activation event. This work provides the first comparison of in-source CID and beam-type CID spectra of emerging synthetic drugs on the same instrument to understand the fragmentation differences between the two techniques and to contribute to the scientific foundations of in-source CID. Electrospray ionization–quadrupole time-of-flight (ESI-Q-TOF) mass spectrometry was used to generate product ion spectra from in-source CID and beam-type CID for a series of well-characterized fentanyl analogs and synthetic cathinones. A comparison between the fragmentation patterns and relative ion abundances for each technique was performed over a range of fragmentor offset voltages for in-source CID and a range of collision energies for beam-type CID. The results indicate that large fragmentor potentials for in-source CID tend to favor higher energy fragmentation pathways that result in both kinetically favored pathways and consecutive neutral losses, both of which produce more abundant lower mass product ions relative to beam-type CID. Although conditions can be found in which in-source CID and beam-type CID provide similar overall spectra, the in-source CID spectra tend to contain elevated noise and additional chemical background peaks relative to beam-type CID.

**KEYWORDS**

forensic science, in-source CID, novel psychoactive substances, seized drugs, tandem mass spectrometry

## 1 | INTRODUCTION

Electron ionization mass spectrometry (EI-MS) is an invaluable tool for the structural identification of unknown organic compounds such as drugs and drug metabolites.[1,2] In particular, the generation of mass spectral databases based on standardized ionization conditions with 70 eV electrons permits remarkable consistency and reproducibility in the spectra collected on different instruments and by different

  

vendors.[3] However, the EI-MS spectra of many organic compounds, such as synthetic cathinones and fentanyl analogs, do not contain abundant molecular ions, which are useful for determining the molecular weight of an unknown.[4,5] An approach to solve this issue is the application of soft ionization sources, such as electrospray ionization (ESI), which results in little to no fragmentation of the $[M + H]^+$ protonated molecules. When used in combination with tandem mass spectrometry (MS/MS), ESI-MS/MS is capable of obtaining both the molecular weight information and structurally informative fragments to help identify compounds and distinguish isobaric and isomeric ions.[6,7]

Tandem mass spectrometry has traditionally involved collisional activation of an isolated precursor ion with a neutral bath gas, commonly termed collision-induced dissociation (CID).[6] The process of CID for beam-type instruments involves 10s–100s of collisions with a neutral gas like nitrogen or argon as the precursor ions pass through the collision cell. In contrast, CID in trapping-type instruments involves 100s of collisions between the stored precursor ions and the neutral bath gas, which is typically helium.[8,9] Trapping-type CID therefore tends to promote lower energy pathways relative to beam-type CID.[6] However, not all instruments include a collision cell or an ion trap, so in-source CID has evolved as a way to accomplish CID in the absence of tandem-MS capabilities or as a cheaper alternative.[10] In-source CID is achieved by manipulating the acceleration voltages as ions transition from the atmospheric pressure ionization source to the high vacuum of the mass analyzer. Manipulation of these voltages causes ions to undergo energetic collisions with residual background gases and, ultimately, fragment. Collision conditions for in-source CID are usually at energies up to hundreds of eV and at pressures on the order of 1 mbar well in excess of low-energy beam-type collisions typically up to 100 eV.[9]

Most of the early in-source CID work was directed towards the fragmentation of macromolecules such as peptides,[11–16] porphyrins,[17] antibiotics,[18] and cytochrome *c*.[19] In addition, comparison studies between in-source CID and tandem mass spectrometry were performed for the analysis of peptides,[20,21] oligosaccharides,[22] and veterinary drugs.[23] More recently, in-source CID applications have expanded to smaller molecules such as opiates,[24] synthetic cathinones,[25] fentanyl analogs,[26] lysergic acid diethylamide (LSD),[27] and inorganic explosives.[28] In-source CID has many monikers, including nozzle/skimmer activation,[11,19] ESI-CID,[3] upfront CID,[3] transport-region CID,[29] and cone-voltage CID.[30] The issue of the reproducibility of in-source CID spectra both within a single instrument[31] and between different instruments has been raised.[32,33] In particular, even with identical source conditions, different source geometries[32,34] or various residual gas compositions[35,36] lead to differences in observed spectra. One approach for generating comparable in-source CID data involves the generation of breakdown curves for several tune compounds on different mass spectrometers.[34,37] Other approaches include the generation of in-source CID libraries based on spectra collected at three different acceleration voltages[38] or through reconstructed spectra composed of data collected at low and high offset voltages.[39] Altering the offset voltage, sometimes referred to as the declustering potential, cone voltage or fragmentor voltage, allows for a tunable degree of fragmentation,[40] which is desirable for library collection.[29]

One widely used instrumental setup for in-source CID is the combination of direct analysis in real time (DART) with high-resolution mass spectrometry (HRMS), such as time-of-flight (TOF) mass spectrometers.[41,42] DART is a rapid, noncontact, ambient ionization technique that produces ions through gas-phase reactions of hot gas effluent from an atmospheric corona-to-glow discharge with reagent molecules and polar or nonpolar analytes.[43,44] The most common applications of DART-TOF with in-source CID are for the analysis of drugs, including synthetic cathinones,[25,45–47] opioids,[48] cannabinoids,[49] stimulants,[50] and botanicals.[51,52] DART with in-source CID and HRMS provides both molecular weight information from the $[M + H]^+$ protonated molecule and structural information from the in-source CID fragments.[53,54] In-source CID can also be employed on quadrupole TOF (Q-TOF) instruments to enable product ion isolation and CID-TOF analysis to achieve pseudo-$MS^3$.[55]

Whereas the use of in-source CID with HRMS has become widely accepted within the drug screening community, there is a void in the forensic science literature for the comparison between in-source CID and conventional beam-type CID. Power et al. examined the similarity between trapping-type CID spectra on an LTQ/Orbitrap instrument and in-source CID spectra collected with a single quadrupole.[45] However, their study is not an apples-to-apples comparison because the mass analyzers were drastically different and might have different mass biases. For example, when comparing the spectra of in-source CID of five compounds on six different instruments, Bristow et al. noted that the geometry of the ionization source has a noticeable effect on the degree of fragmentation and product ion distributions.[32] For the purpose of the present study, we kept the ESI source geometry and TOF detection constant. The only variables that changed were whether the ions were fragmented using in-source CID or beam-type CID and slight shifts in fragmentor voltage based on optimized precursor transmission prior to beam-type CID. Although we have made some comparisons between in-source CID of ESI- and DART-generated precursor ions, those results are beyond the scope of the current work.

The goal of this study is to qualitatively analyze the product ion spectra generated with in-source CID and beam-type CID for a series of fentanyl analogs and synthetic cathinones that have been previously well-characterized.[56,57] The Q-TOF mass spectrometer allows for the collection of both in-source CID product ion spectra and beam-type CID product ion spectra by switching between full-scan mode and MS/MS mode, which involves the isolation of a desired precursor ion and the application of an optimized collision energy. This instrumental setup allows for the comparison of mass spectra generated under conditions that are as similar as possible.[41] This study provides the forensic science community with empirical comparisons between these two commonly employed fragmentation techniques to help solidify the basis for in-source CID as a technique and for comparing in-source CID spectra with spectra collected on beam-type instruments. The strong similarities suggest that, in general,

fragmentation mechanisms from beam-type CID studies can be applied to in-source CID spectra. Finally, with the increasing interest in the application of HRMS for rapid drug screening, this study provides insight into the benefits and drawbacks of in-source CID relative to beam-type CID and the implications for forensic practitioners with an emphasis on emerging synthetic drugs.

## 2 | METHODS

### 2.1 | Sample preparation

Four *N*-alkylated synthetic cathinones and two fentanyl analog standards were purchased through Cerilliant (Round Rock, TX, USA) including methcathinone-$d_3$ (*N*-alkyl deuterated), diethylpropion-$d_{10}$ (*N*-alkyl deuterated), pentylone-$d_3$ (*N*-alkyl deuterated), dibutylone-$d_3$ (alkyl deuterated), alfentanil, and furanylfentanyl. Two additional fentanyl analogs were purchased through Cayman Chemical (Ann Arbor, MI, USA) including *ortho*-methylfentanyl and β-hydroxythiofentanyl-$d_5$ (perdeuterated on the amide). Table S1 provides the corresponding protonated molecular structure and exact masses for all compounds in this study. The synthetic cathinones were chosen based on the desire to have varying molecular weights and both 2° and 3° amines. The fentanyl analogs were chosen to represent analogs with substitutions on different positions of the core fentanyl structure, consistent with our previous work on the influence of chemical modifications on the fragmentation behavior of fentanyl analogs.[56] The incorporation of deuterated analogs provides in-source CID data for compounds that may be used by others as internal standards for quantitative analyses. Also deuterated compounds are available as DEA-exempt preparations and help confirm proposed fragmentation pathways. All standards were prepared in a solution of 49% high-performance liquid chromatography (HPLC) grade methanol, 49% distilled water, and 2% acetic acid to a final concentration of approximately 100 ppm. The HPLC grade methanol was supplied by Fisher Scientific (Palo Alto, CA, USA) and the acetic acid was supplied by Acros Organics (Palo Alto, CA, USA).

### 2.2 | Instrumentation

#### 2.2.1 | Agilent Technologies 6538 UHD Accurate-Mass Q-TOF

A dual-ESI source was operated with a spray voltage of 3500 V and a 300 °C nitrogen drying gas flow of 5 L/min and a nebulizer flow of 30 psig. Direct infusion of standards was accomplished with a 5 μL/min flow rate. In-source CID spectra were collected using a skimmer setting of 65 V and fragmentor settings varying from 95 to 300 V to produce a range of in-source CID spectra. Likewise, the collision energy used for the beam-type CID portion of this study was varied from 15 to 35 eV to provide a range of beam-type CID spectra. All beam-type CID spectra were collected with an isolation width of 1.3 Da, and the scan range was from *m/z* 50 to a value that exceeded the molecular mass by ~50 Da. Ultra-pure nitrogen was used for the collision gas purchased through Matheson TRIGAS (Fairmont, WV, USA).

#### 2.2.2 | Thermo Scientific Velos Pro linear ion trap

Supporting trapping-type CID experiments were also collected using a Thermo Scientific Velos Pro linear ion trap (LIT) mass spectrometer with a heated-electrospray ionization (HESI) source at 50 °C. Again, direct infusion of standards was achieved with a flow rate of 5 μL/min. The spray voltage was 4000 V with the nitrogen sheath gas flow set to 8 arbitrary units, and the nitrogen auxiliary flow was set to five arbitrary units. The mass spectrometer capillary temperature was set to 275 °C. The scan range and normalized collision energy (NCE) were specific for each compound and are labeled with each mass spectrum. The bath gas was ultra-pure helium from Matheson TRIGAS (Fairmont, WV, USA).

### 2.3 | Data analysis

MassHunter Qualitative Analysis B.05.00 and Xcalibur 2.0.0.48 software were used for the Agilent Q-TOF and Thermo Scientific LIT data analysis, respectively. All compounds in this study were analyzed with both the Q-TOF and LIT to verify the fragmentation pathways and provide a comparison between in-source CID, beam-type CID, and trapping-type CID. Spectra are provided in the manuscript, and supplemental material and are available on request. Microsoft Excel version 14 (Microsoft, Redmond, WA, USA) was used for the mass spectral plots, and ChemDraw 16.0 (PerkinElmer, Waltham, MA, USA) was used to create the embedded structures.

### 2.4 | Spectral interpretation

This study provides described below involves at least one beam-type CID spectrum and at least one in-source CID spectrum, and the figure caption provides extensive information about the experimental conditions used to collect each spectrum. In addition, Table S2 provides comprehensive information about the elemental formula and exact mass for each ion discussed in text.

## 3 | RESULTS AND DISCUSSION

### 3.1 | Fentanyl analogs

Figure 1 shows a comparison between beam-type CID and in-source CID spectra for *ortho*-methylfentanyl. The $[M + H]^+$ protonated precursor for *ortho*-methylfentanyl is observed at *m/z* 351.2437 (<1 ppm error) in Figure 1A. A sodiated adduct ($[M + Na]^+$) is also

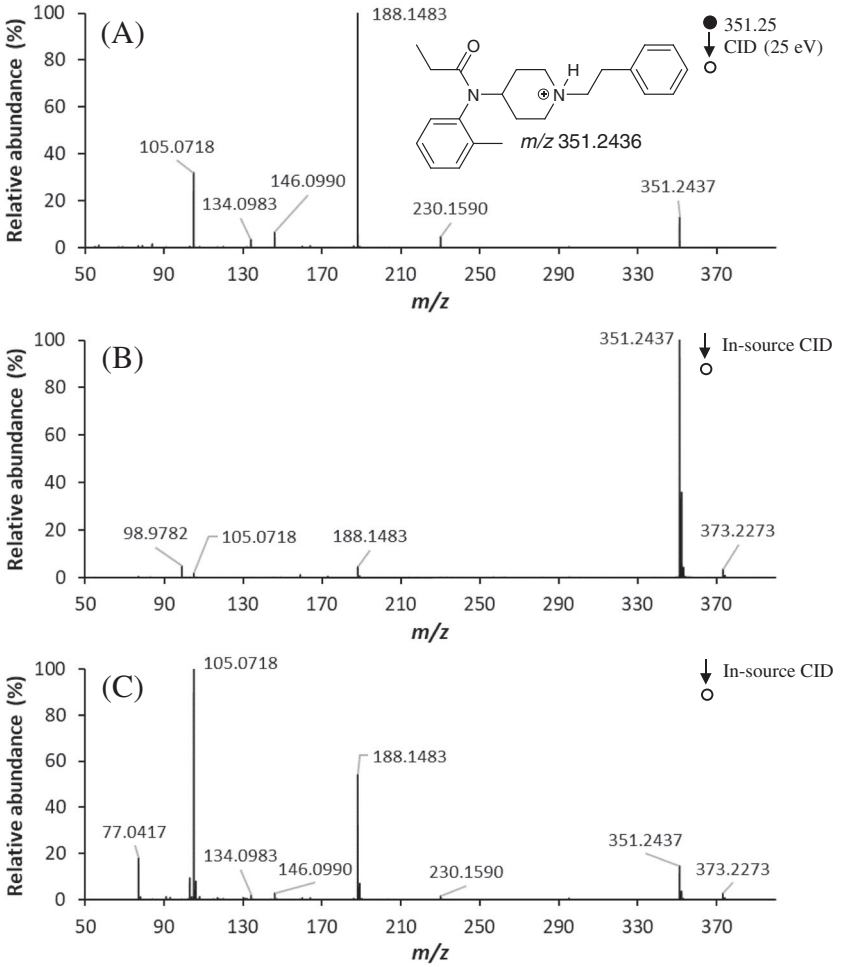


**FIGURE 1** Comparison of beam-type CID (top) and in-source CID (middle and bottom) for protonated *ortho*-methylfentanyl. For all spectra, the skimmer setting was held at 65 V. For beam-type CID, the fragmentor setting was 250 V with a collision energy of 25 eV. For in-source CID, the fragmentor settings were 175 and 300 V, for (B) and (C), respectively, with the collision energy set to 0 eV

evident at *m/z* 373.2273 (5 ppm error) in Figures 1B,C. Figure 1A shows the beam-type CID spectrum with product ions at *m/z* 230.1590 (20 ppm error), *m/z* 188.1483 (23 ppm error), *m/z* 146.0990 (14 ppm error), *m/z* 134.0983 (10 ppm error), and *m/z* 105.0718 (13 ppm error), which is consistent with our previous work.[56] For *ortho*-methylfentanyl, all of the product ions formed in beam-type CID are found in the in-source CID spectrum, but the reverse is not true. The in-source CID spectrum shows a phenylium peak at *m/z* 77.0417 that is negligible in the beam-type CID spectrum. The phenylium ion at *m/z* 77.0417 either derives from a higher energy direct cleavage of the precursor or from a simple neutral loss of $C_2H_4$ from the phenylethyl ion at *m/z* 105.0718.

The fragmentor setting of 175 V in Figure 1B provided inefficient fragmentation and weak product ion signals. Low-abundance in-source CID product ions are observed at *m/z* 188.1483 (23 ppm error) and *m/z* 105.0718 (13 ppm error). The phenethylpiperidine ion expected at *m/z* 188.1439 has been described extensively for fentanyl, including the presence of isobaric species formed through the loss of the *N*-phenylpropanamide moiety directly or through the loss of methylketene followed by the loss of aniline.[58,59]

The presence of the phenethylpiperidine ion at *m/z* 188.1483 and the phenylethyl ion at *m/z* 105.0718 are consistent with previous literature on in-source CID of fentanyl and fentanyl analogs.[26] The actual structure of the fragment at *m/z* 105.0718 could also be a methyl-tropylium or phenonium ion.[60] The ion at *m/z* 98.9782 in Figure 1B has a negative mass defect that is not consistent with any viable fragment of *ortho*-methylfentanyl and must therefore derive from an impurity or background contamination. The same ion was observed in other full-scan and low energy in-source CID spectra, and the most reasonable identity—based on the likelihood of occurrence and accurate mass—is $H_3SO_4^+$ (35 ppm error). However, the chemical identity of the ion at *m/z* 98.9782 has not been confirmed.

In contrast to the low energy in-source CID spectrum in Figure 1B, the higher energy in-source CID spectrum in Figure 1C provides more abundant low mass ions, including the readily observed phenylium product ion at *m/z* 77.0417 (34 ppm error). As expected, larger fragmentor voltages enhanced the fragmentation efficiencies and decreased the precursor ion abundance.

The $[M + H]^+$ protonated precursor of furanylfentanyl is observed at *m/z* 375.2134 (16 ppm error) in Figure 2. A sodiated adduct ($[M + Na]^+$) is also evident at *m/z* 397.1914 (6 ppm error) in Figures 2B,C. In contrast to Figure 1, the observed product ion distribution is noticeably absent of any intermediate of significant abundance between the precursor ion and the phenethylpiperidine ion at *m/z* 188.1471. At higher energies, the electron-withdrawing characteristics of the furyl group for furanylfentanyl tend to favor the

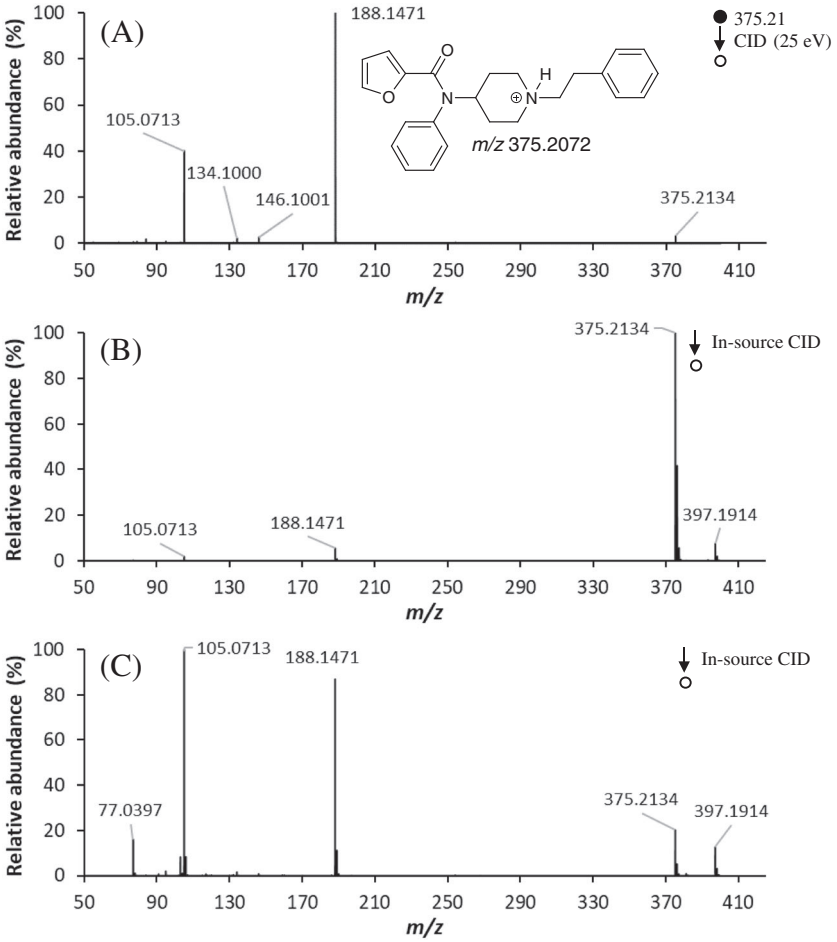


**FIGURE 2** Comparison of beam-type CID (top) and in-source CID (middle and bottom) for protonated furanylfentanyl. For all spectra, the skimmer setting was held at 65 V. For beam-type CID, the fragmentor setting was 225 V with a collision energy of 25 eV. For in-source CID, the fragmentor settings were 165 and 285 V, for (B) and (C), respectively with the collision energy set to 0 eV

direct loss of the *N*-phenylalkylamide moiety and drive facile secondary fragmentation.[56] The product ions at *m/z* 188.1471 (17 ppm error), *m/z* 146.1001 (22 ppm error), *m/z* 134.1000 (24 ppm error), and *m/z* 105.0713 (9 ppm error) are consistent with the previous literature.[58,61,62]

Figure 2B provides a low abundance of product ions because the fragmentor offset is too low to achieve efficient CID. The poor spectrum shows that it is difficult or impossible to obtain low-energy in-source CID spectra with acceptable CID efficiencies at a fragmentor voltage of 175 V. The presence of the phenethylpiperidine ion at *m/z* 188.1471 (17 ppm error) and phenylethyl ion (or phenonium or methyl-tropylium ion[60]) at *m/z* 105.0713 (9 ppm error) has been reported previously in literature for furanylfentanyl.[63] As the fragmentor voltage is increased, the low-mass product ions increase in abundance relative to the precursor ion signal (Figure 2C).

One notable difference between the in-source CID spectrum and beam-type CID spectrum of furanylfentanyl is the abundance of the phenylium ion at *m/z* 77.0391 for beam-type CID, which, as discussed above, could be a higher energy direct cleavage product or a consecutive fragment. The accurate mass measurements indicate that the elemental composition at *m/z* 105.0713 is $C_8H_9^+$, which is consistent with a phenylethyl ion (or methyl-tropylium or phenonium ion[60]) structure from the *N*-phenylethyl group on the piperidine nitrogen. The expected pathway to the phenylethyl cation is through charge-directed inductive cleavage from the 1-(2-phenylethyl)-2,3,4,5-tetrahydropyridium ion at *m/z* 188.1471 to form the phenylethyl cation at *m/z* 105.0713.[58,59]

Figure 3 shows a comparison between the beam-type CID spectra and in-source CID spectrum for alfentanil collected at different collision energies. Under the in-source CID conditions, there is a wealth of product ion information in addition to the presence of the $[M + H]^+$ protonated precursor at *m/z* 417.2628 (3 ppm error) and the $[M + Na]^+$ precursor at *m/z* 439.2480 (11 ppm error). The major in-source CID generated product ions at *m/z* 385.2381 (8 ppm error), *m/z* 314.1892 (7 ppm error), *m/z* 268.1831 (22 ppm error), *m/z* 197.1296 (3 ppm error), and *m/z* 165.1064 (23 ppm error) are all in agreement with the beam-type CID spectra. The observed product ions are consistent with previous literature for substitution at the 4-position of the piperidine ring, as seen by the neutral losses of methanol (i.e., at *m/z* 385.2381) and *N*-phenylpropanamide (i.e., at *m/z* 268.1831).[56,64]

Figure 4 compares spectra from beam-type CID and in-source CID of β-hydroxythiofentanyl-$d_5$. Unlike the other fentanyl analogs, the sodiated adduct ($[M + Na]^+$) was more abundant than the protonated adduct ($[M + H]^+$) in the full scan mass spectra of β-hydroxythiofentanyl-$d_5$. For consistency with the other analogs, the less-abundant protonated precursor was isolated for beam-type CID, which provided slightly inferior signal-to-noise ratios in the low mass

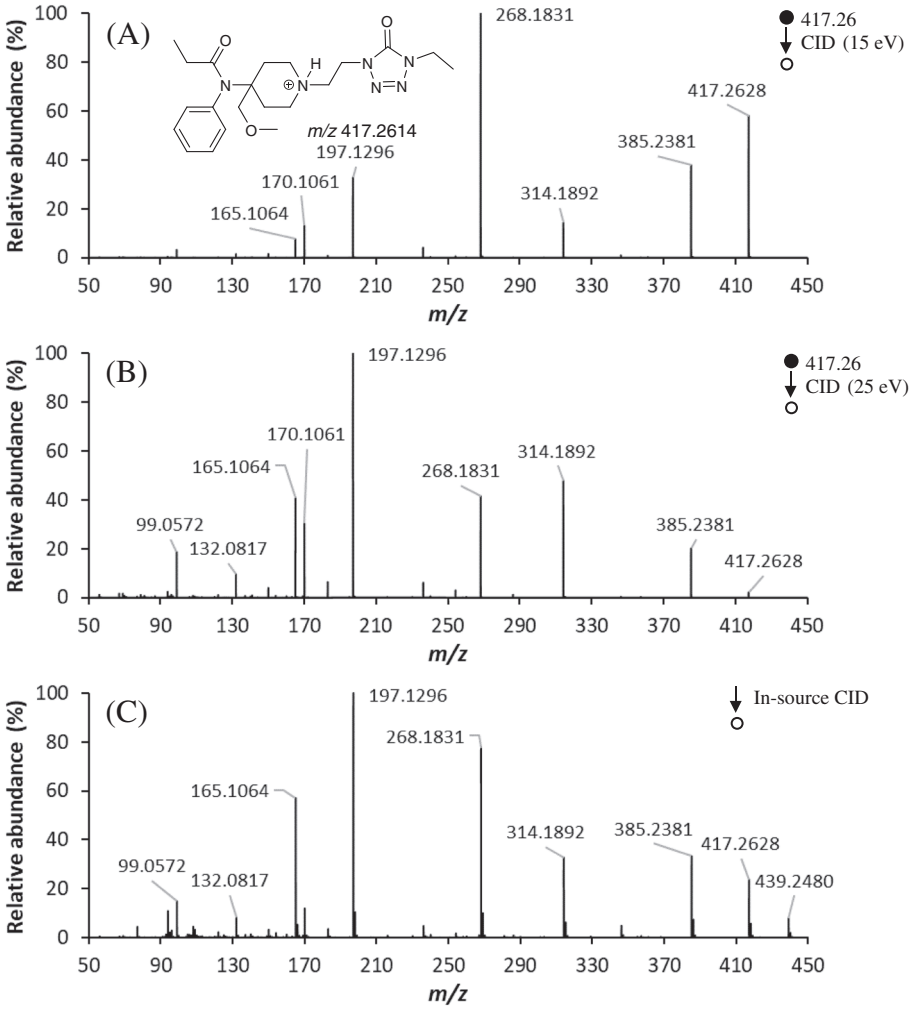


**FIGURE 3** Comparison of beam-type CID (top and middle) and in-source CID (bottom) for protonated alfentanil. For all spectra, the skimmer setting was held at 65 V. For beam-type CID, the fragmentor setting was 225 V with collision energies of 15 and 25 eV for (A) and (B), respectively. For in-source CID, the fragmentor setting was 285 V with a collision energy of 0 eV

region of the spectrum relative to the other analogs. As is typical for both beam-type and in-source CID, the product ion distribution shifts towards lower masses at higher collision energies (Figure 4B) relative to lower collision energies (Figure 4A) because of sequential neutral losses and access to pathways with higher dissociation energies. The base peak of Figure 4A is *m/z* 346.2021, which is consistent with the neutral loss of $H_2O$ from the $[M + H]^+$ protonated precursor. This intermediate ion at *m/z* 346.2021 fragments into the products at *m/z* 286.1511 and *m/z* 192.0895, which have been described previously.[56]

Figure 4C contains both the $[M + H]^+$ protonated precursor at *m/z* 364.2114 (3 ppm error) and the $[M + Na]^+$ precursor at *m/z* 386.1955 (9 ppm error). The fragmentor setting of 285 V provides sufficient collisional activation to generate multiple diagnostic product ions, including *m/z* 346.2021 (7 ppm error), *m/z* 286.1511 (8 ppm error), *m/z* 210.0982 (14 ppm error), *m/z* 192.0895 (26 ppm error), *m/z* 111.0295 (23 ppm error), and *m/z* 97.0135 (25 ppm error).

### 3.1.1 | Discussion for fentanyl analogs

The comparison between in-source CID and beam-type CID for fentanyl analogs reveals a great deal of similarity between the observed product ion spectra. In general, the abundant product ions are conserved between the two activation techniques, and there is general agreement between the spectra. A careful assessment also reveals that the in-source CID spectra tend to be noisier relative to the beam-type CID spectra, and that there are usually distinguishable differences in the relative abundance of selected product ions, which is observed as both ion drop-in and ion drop-out. For example, the in-source CID spectrum of *ortho*-methylfentanyl in Figure 1B shows the presence of a product ion at *m/z* 98.9782 that is not present in the beam-type CID spectrum in Figure 1A. We interpret this observation to imply that *m/z* 98.9782 must arise from an alternative precursor than *ortho*-methylfentanyl because there are no reported pathways to this fragment mass in the literature. Furthermore, the product ion at *m/z* 98.9782 is not present in the higher energy in-source CID spectrum (Figure 1C), which indicates that the ion has probably undergone collisional activation in Figure 1C. Such observations are significant because the fentanyl analogs in this study were standards and thus have minimal background interferences, unlike casework samples that would contain mixtures of drugs, cutting agents, adulterants or complex biological matrices. Others have noted that in-source CID struggles with dilute or impure samples[65] and that relative ion abundances are likely to fluctuate from the day-to-day differences in the

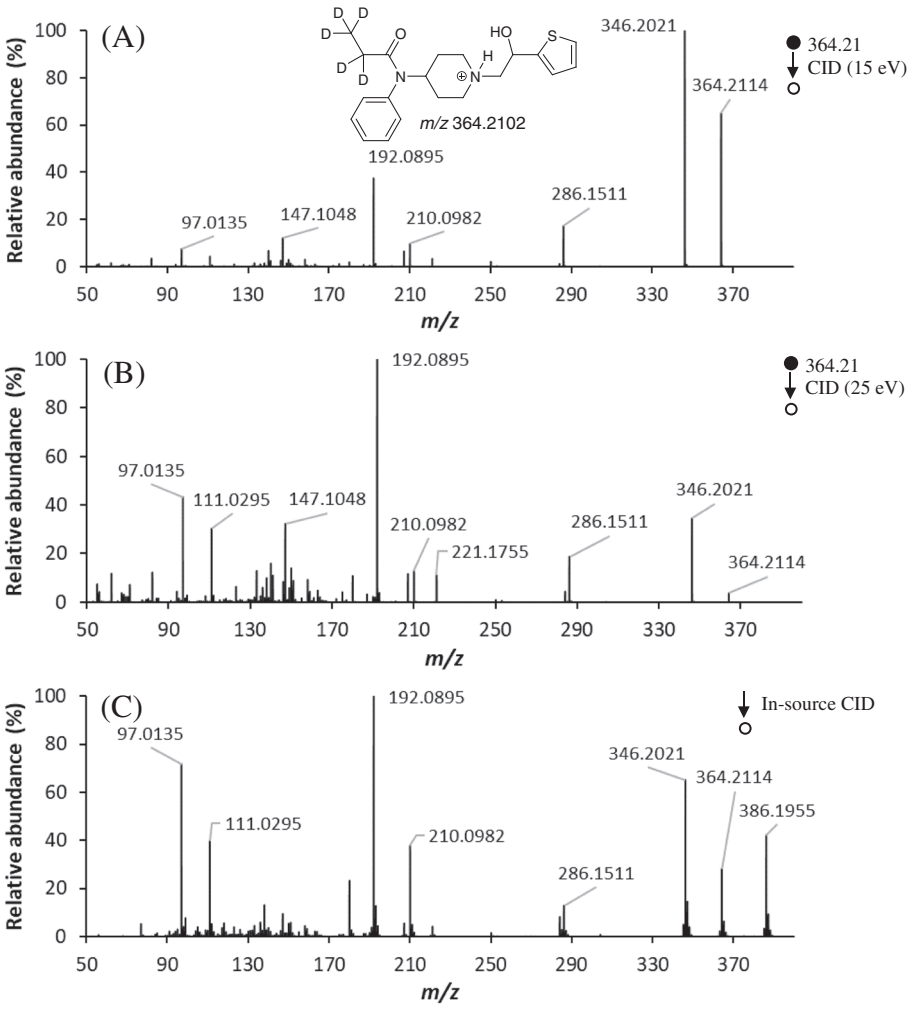


**FIGURE 4** Comparison of beam-type CID (top and middle) and in-source CID (bottom) for protonated β-hydroxythiofentanyl-$d_5$. For all spectra, the skimmer setting was held at 65 V. For beam-type CID, the fragmentor setting was 225 V with collision energies of 15 and 25 eV, for (A) and (B), respectively. For in-source CID, the fragmentor setting was 285 V with a collision energy of 0 eV

composition of the residual gases in the source region during in-source CID. However, reproducibility studies indicate fragment ion abundances typically have a standard deviation of about 5% relative to the mean abundance.[3,37]

When comparing in-source CID and beam-type CID in Figures 1–3, subtle differences in the relative abundance of peaks with comparable *m/z* values indicate fundamental differences in internal energy deposition rates rather than mass bias or other effects if the peaks were spaced further apart. For example, the in-source CID spectrum of alfentanil (Figure 3C) shows a peak at *m/z* 170.1061 (expected at *m/z* 170.1042 for $C_6H_{12}N_5O^+$; 12 ppm error) that is only ~20% the abundance of the fragment at *m/z* 165.1064 (expected at *m/z* 165.1027 for $C_9H_{13}N_2O^+$; 22 ppm error). At the higher beam-type CID amplitude of 25 eV in Figure 3B, the peak at *m/z* 170.1061 is ~80% the abundance of the peak at *m/z* 165.1064. In contrast, the lower energy spectrum in Figure 3A—with a collision energy of 15 eV—provides a peak at *m/z* 170.1061 that is 130% the abundance than the peak at *m/z* 165.1064. In the slow heating conditions of trapping-type CID, the same peak at *m/z* 170 was ~140% the abundance of the peak at *m/z* 165 (Supporting Information). The ratio of abundances at *m/z* 165:170 therefore varies from ~0.75:1 for trapping-type CID and low-energy beam-type CID to 1.25:1 at higher energy beam-type CID and ~5:1 for in-source CID. Based on $MS^n$ data collected on the LIT, the product ions at *m/z* 170 and *m/z* 165 form via consecutive neutral losses through several different fragmentation pathways, including the abundant intermediate ion at *m/z* 268, which is formed through the loss of neutral *N*-phenylpropanamide from the protonated precursor. From the intermediate ion at *m/z* 268, the product ion at *m/z* 165 forms through the loss of $C_2H_5N_3$ (i.e., *m/z* 197) followed by the loss of methanol, whereas the product ion at *m/z* 170 forms through the loss of $C_6H_{10}O$ from a piperidine ring cleavage. The abundance of *m/z* 165 correlates with the abundance of its precursor at *m/z* 197, with both product ions (*m/z* 165 and *m/z* 197) gaining prominence at elevated CID energies in beam-type CID (Figure 3B) relative to trapping-type CID (Supporting Information). Based on the comparison between in-source CID (Figure 3C), beam-type CID (Figures 3A,B) and trapping-type CID (Supporting Information), in-source CID provides the greatest relative abundance of peaks at *m/z* 165 and 197. Because the relative energies and activation barriers for these pathways are not known, we can only speculate that the product ion at *m/z* 170 has a lower activation barrier than *m/z* 165.

In the slow heating conditions of trapping-type CID of β-hydroxythiofentanyl-$d_5$, the peak at *m/z* 207 was slightly more

abundant than the peak at *m/z* 210 (Supporting Information). The beam-type CID spectra in Figures 4A,B provide an accurate mass of *m/z* 207.1540 (expected at *m/z* 207.1540 for $C_{13}H_{11}D_5NO^+$; <1 ppm error), which forms through competing pathways through either the loss of the hydroxymethylthiol to form the intermediate at *m/z* 250 followed by the loss of a $C_2NH_5$ neutral from the piperidine ring or through the loss of $H_2O$, followed by the loss of the deuterated *N*-phenylpropanamide moiety. These pathways were confirmed in $MS^3$ experiments with the linear ion trap.[56] In contrast to consecutive, low-energy rearrangements leading to *m/z* 207.1540, the product ion at *m/z* 210.0982 has an elemental composition $C_{11}H_{16}NOS^+$ (expected at *m/z* 210.0952; 14 ppm error) and forms via cleavage between the aniline nitrogen and the piperidine ring in a single step, so it is probably kinetically favored. The beam-type CID spectra show similar abundances for the two product ions at *m/z* 207.1540 and *m/z* 210.0982, whereas the in-source CID spectrum in Figure 4C shows that the peak at *m/z* 210.0982 is considerably more abundant (by a factor of ~7×). Again, these findings show that the in-source CID spectrum in Figure 4A provides more rapid heating and kinetically favored single-cleavage product ions relative to beam-type CID experiments or the trapping-type CID experiments of our previous work.[56]

## 3.2 | Synthetic cathinones

Figure 5 shows the product ion spectra for methcathinone-$d_3$ collected with beam-type CID and in-source CID. The perdeuterated methyl group is in the *N*-alkyl position. Methcathionone-$d_3$ is a 2° amine, *N*-alkylated, synthetic cathinone and has a relatively small molecular weight compared with other cathinones and fentanyl analogs. Figure 5A shows the beam-type CID spectrum with the base peak at *m/z* 134.0960 (30 ppm error). Figure 5B shows the dominant loss of $H_2O$ observed at *m/z* 149.1160 (4 ppm error) from the $[M + H]^+$ protonated precursor at *m/z* 167.1295 (21 ppm error). This fragmentation behavior is consistent with previous literature for *N*-alkylated synthetic cathinones.[4,66–69] Note that, unlike the fentanyl analogs, neither methcathinone-$d_3$ nor any of the other synthetic cathinones show sodiated adducts ($[M + Na]^+$) in the full-scan mass spectra. The lack of sodiation likely is related to the relative sodium affinity of synthetic cathinones relative to fentanyl analogs, but could also be related to differences in the sodium impurities of the purchased standards.

Figure 5C shows that, at higher acceleration potentials of in-source CID, the product ion distribution shifts towards lower

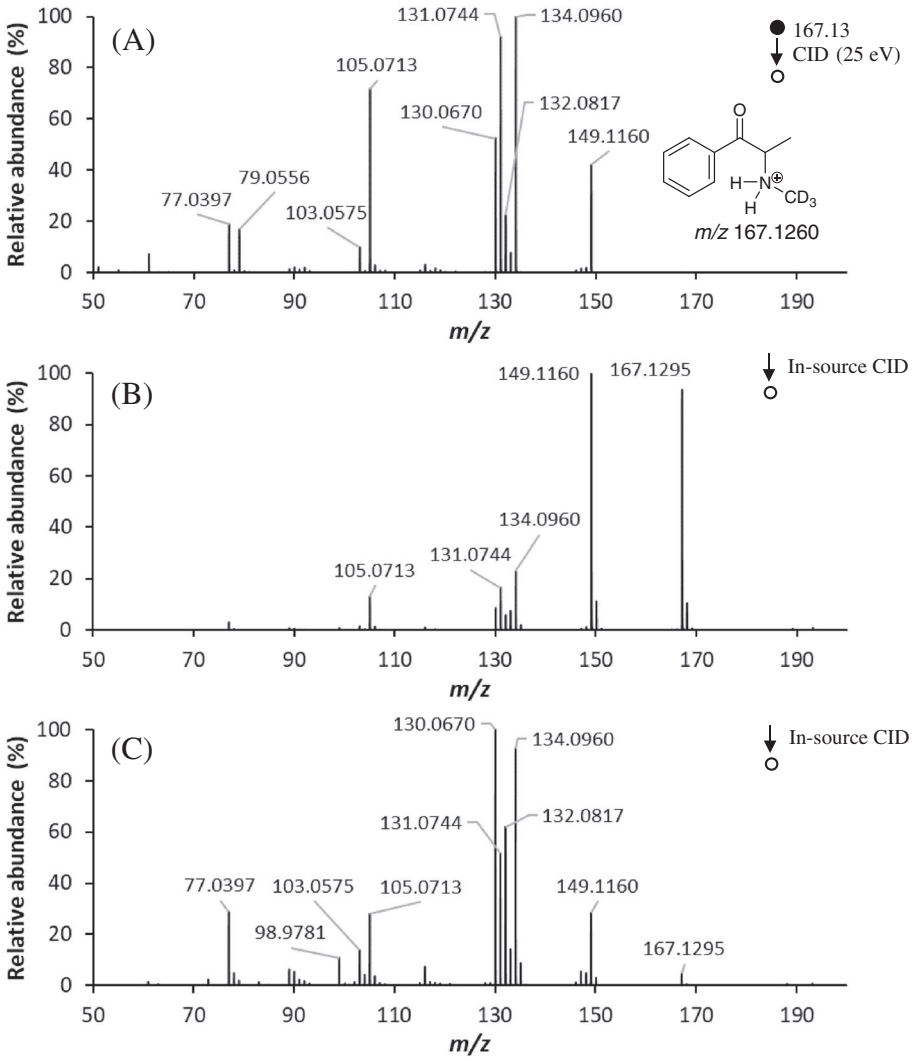


**FIGURE 5** Comparison of beam-type (CID) (top) and in-source CID (middle and bottom) for protonated methcathinone-$d_3$. For all spectra, the skimmer setting was held at 65 V. For beam-type CID, the fragmentor setting was 175 V with a collision energy of 25 eV. For in-source CID, the fragmentor settings were 175 and 255 V, for (B) and (C), respectively with the collision energy set to 0 eV

masses, likely because the smaller ions are thermodynamically more stable than large ions and have higher dissociation thresholds. The ions at smaller *m/z* values could also derive from multiple neutral losses. The major product ions observed from beam-type CID are consistent with the major product ions observed for in-source CID, including product ions at *m/z* 149.1160 (4 ppm error), *m/z* 134.0960 (30 ppm error), *m/z* 131.0744 (8 ppm error), and *m/z* 105.0713 (9 ppm error). Two product ions of note are *m/z* 134.0920 and *m/z* 131.0744, which are formed through the loss of a radical methyl group ($^{\bullet}CH_3$) from the aliphatic chain and a radical deuterated methyl group ($^{\bullet}CD_3$) from the *N*-alkyl chain, respectively. The presence of even-electron intermediates fragmenting into odd-electron product ions has been reported before for *N*-alkylated synthetic cathinones.[55,57,66]

Similar to the fentanyl analogs, the in-source CID spectra and beam-type CID spectra occasionally show significant differences in relative ion abundances for peaks that are close together and therefore these differences in abundance are not caused by mass bias. For example, in the beam-type CID spectrum of methcathinone-$d_3$ in Figure 5A, the peak at *m/z* 131.0744 is ~39% more abundant than the peak at *m/z* 130.0670. However, although the higher energy in-source CID spectrum in Figure 5C shares overall spectral similarity with the beam-type CID spectrum, the relative abundance of the peak at *m/z* 131.0744 is only ~50% the abundance of the peak at *m/z* 130.0670. Previous work indicates that the product ion at *m/z* 131.0744 is a distonic radical cation formed via the loss of the methyl group from the *N*-alkyl position.[55,57,66] Without the benefit of isotope labeling, Bijlsma et al. assumed that the methyl radical was lost from the aliphatic chain.[70] However, per-deuteration on the *N*-methyl group shows that the intermediate at *m/z* 149.1160 can evidently lose either $^{\bullet}CH_3$ (15 Da) from the aliphatic chain to form the product at *m/z* 134.0960 or $^{\bullet}CD_3$ (18 Da) from the *N*-methyl position to form the product at *m/z* 131.0744 with approximately equal preference.[57] The formation of an alkylphenone at *m/z* 133.0960 through the loss of the *N*-methyl moiety is generally unfavorable in all the spectra, whereas the additional radical loss of $^{\bullet}H$ (1 Da) from the distonic radical intermediate at *m/z* 131.0744 to give the even-electron product ion at *m/z* 130.0670 is kinetically favored at higher internal energies, as demonstrated by its greater abundance in the highest energy in-source CID conditions.

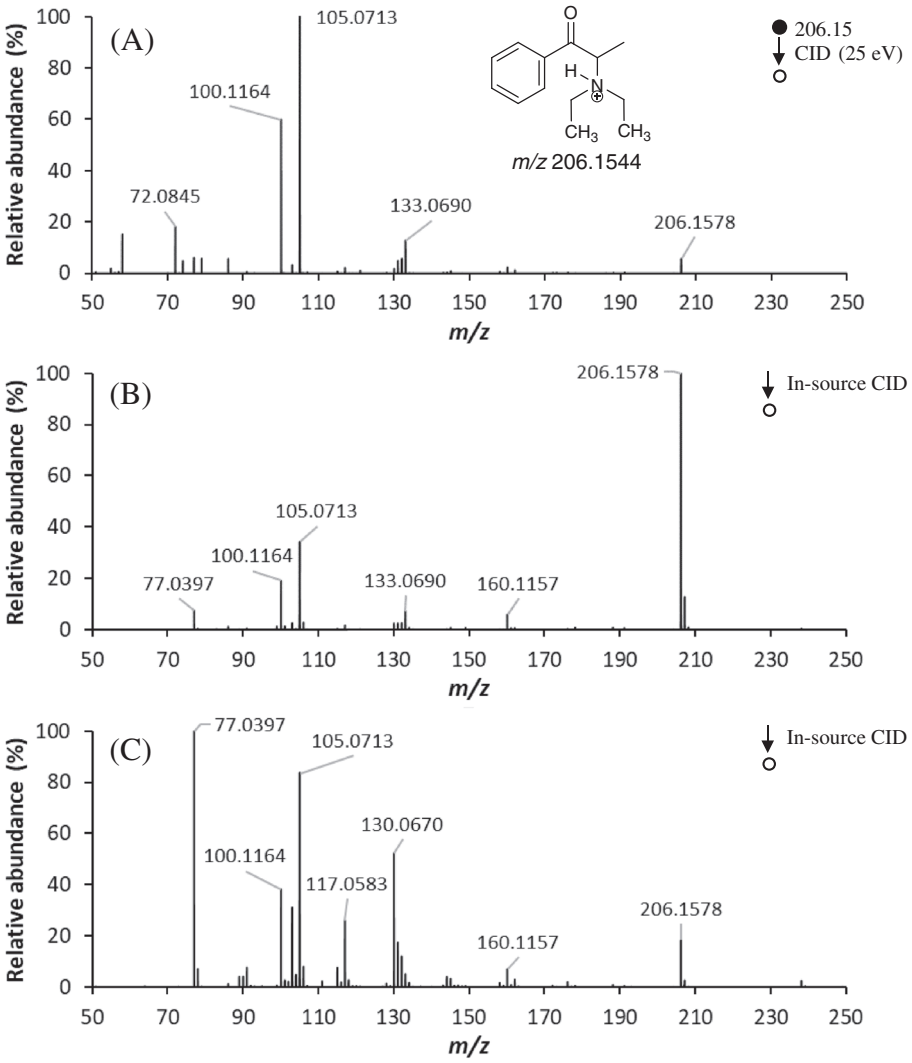


**FIGURE 6** Comparison of beam-type (CID) (top) and in-source CID (middle and bottom) for protonated diethylpropion. For all spectra, the skimmer setting was held at 65 V. For beam-type CID, the fragmentor setting was 225 V with a collision energy of 25 eV. For in-source CID, the fragmentor settings were 225 and 285 V, for (B) and (C), respectively, with the collision energy set to 0 eV

Like methcathinone-$d_3$, diethylpropion also has a relatively small molecular weight, but diethylpropion is a 3° amine, *N*-alkylated, synthetic cathinone. Figure 6 provides a comparison between beam-type CID and in-source CID for diethylpropion. The in-source CID spectra in Figures 6B,C reveal the conversion of the $[M + H]^+$ protonated molecule at *m/z* 206.1578 (16 ppm error) to product ions at *m/z* 160.1157 (19 ppm error), *m/z* 133.0690 (28 ppm error), *m/z* 105.0713 (9 ppm error), *m/z* 100.1164 (38 ppm error), and *m/z* 77.0397 (8 ppm error), and the most abundant product ions at *m/z* 105.0713 and *m/z* 100.1126 are consistent with previous literature.[71]

The product ions at *m/z* 133.0690 and *m/z* 100.1164 are of particular importance because these product ions correspond with the formation of an alkylphenone and iminium cation, respectively. Our previous work with *N*-alkylated synthetic cathinones demonstrated that, whereas 2° amines favor the loss of water, 3° amines favor the formation of alkylphenones and a corresponding iminium counter ion.[57] The common phenylethyl ion at *m/z* 105.0713 and phenylium ion at *m/z* 77.0397 were also identified.[57] In general, the in-source CID product ions are in agreement with the beam-type CID product ions at a collision energy of 25 eV (Figure 6A). One exception is the presence of the product ion at *m/z* 72.0845 (44 ppm error) in the beam-type CID spectrum, which arises through consecutive fragmentation from the intermediate at *m/z* 100.1164. One explanation for the low abundance at nominal *m/z* 72 in the in-source CID spectrum is that kinetic-based products are more competitive relative to this product of sequential neutral losses. Another reason for the absence of nominal *m/z* 72 in the in-source CID spectra could be due to instrumental discrimination against low mass ions at elevated fragmentor settings. In our experience, nominal *m/z* 77 was the lowest mass product ion of any significant abundance from dozens of in-source CID spectra, even though the scan range started at *m/z* 50 in all cases and the beam-type CID spectra often contained fragments between nominal *m/z* 50–77.

Figure 7 shows the beam-type CID and in-source CID mass spectra for pentylone-$d_3$, which is a relatively large molecular weight, 2° amine, *N*-alkylated, synthetic cathinone. Figure 7C shows a significant portion of the $[M + H]^+$ protonated precursor ion at *m/z* 239.1530 (25 ppm error) is converted to product ions through collisional activation. The common product ions observed in Figure 7C include *m/z* 221.1395 (13 ppm error), *m/z* 191.1275 (8 ppm error), *m/z* 178.0843 (14 ppm error), *m/z* 135.0465 (14 ppm error), and *m/z* 89.1171 (19 ppm error), among others.

The product ion at *m/z* 221.1395 is formed through the loss of $H_2O$, and the product ion at *m/z* 178.0843 is formed by an additional

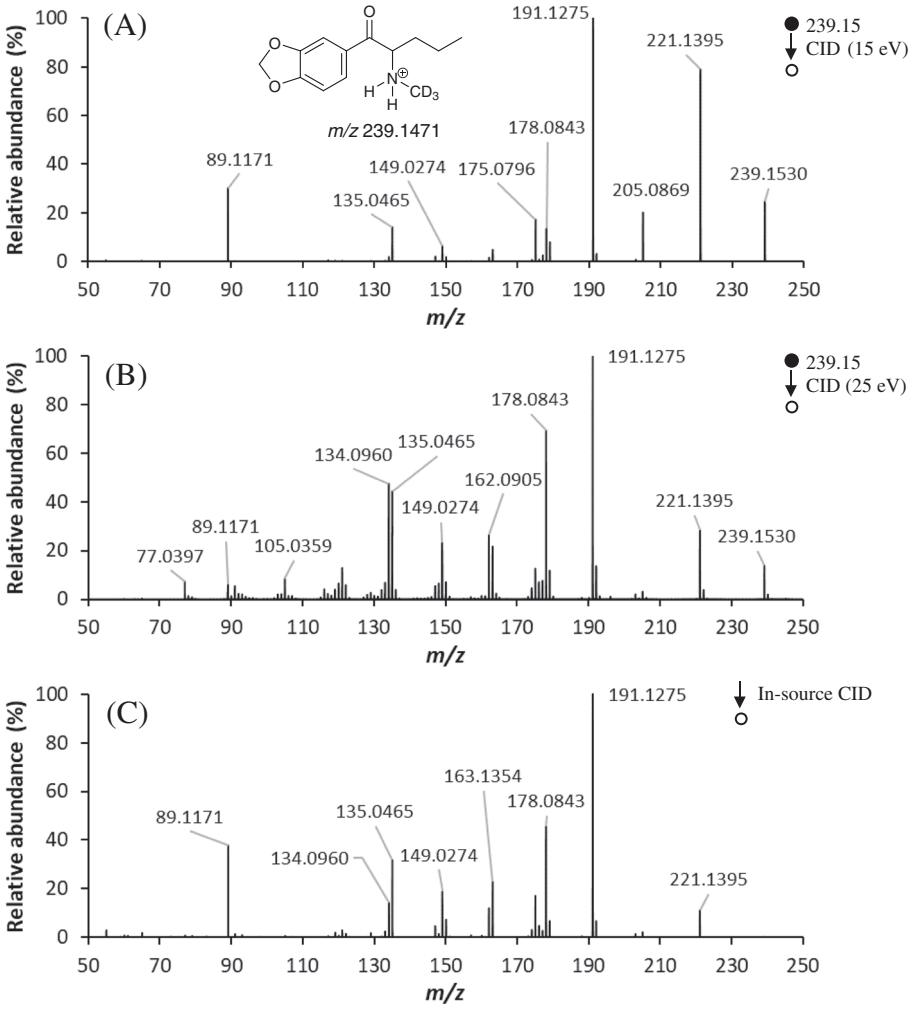


**FIGURE 7** Comparison of beam-type (CID) (top and middle) and in-source CID (bottom) for protonated pentylone-$d_3$. For all spectra, the skimmer setting was held at 65 V. For beam-type CID, the fragmentor setting was 175 V with collision energies of 15 and 25 eV, for (A) and (B), respectively. For in-source CID, the fragmentor setting was 255 V with a collision energy of 0 eV

loss of a propyl radical ($^{\bullet}C_3H_7$). As mentioned above, the radical losses from even-electron precursors are commonly observed in tandem mass spectra of *N*-alkylated synthetic cathinones.[55,57,66] Likewise, the product ion at *m/z* 191.1275 occurs through the loss of formaldehyde ($CH_2O$), which is typical for methylenedioxy-containing synthetic cathinones.[4,72,73] Finally, the product ions at *m/z* 135.0465 and *m/z* 89.1171 are consistent with the methylenedioxy-substituted tropylium ion and the deuterated iminium ion. As the collision energy is increased from 15 eV in Figure 7A to 25 eV in Figure 7B, the corresponding product ion spectrum shifts to lower mass ions through higher energy fragmentation events, which allows for the generation of additional product ions, such as those at *m/z* 105.0359 (8 ppm error) and *m/z* 77.0397 (48 ppm error). As with the fentanyl analogs, we cannot be sure whether the phenylium ion at *m/z* 77.0397 forms via direct cleavage or via consecutive cleavages. Whereas a potential pathway for the fentanyl analogs was via the loss of $C_2H_4$ from the phenylethyl ion at *m/z* 105.0713, a potential intermediate for the cathinone analogs is via the loss of CO from the benzoyl ion at *m/z* 105.0359.

Dibutylone-$d_3$ has the same molecular mass as pentylone-$d_3$ (238 g/mol), but dibutylone-$d_3$ is a 3° amine, *N*-alkylated, synthetic cathinone. The in-source CID spectrum (Figure 8C) reveals efficient conversion of the $[M + H]^+$ protonated precursor at *m/z* 239.1519 (20 ppm error) to product ions. The product ions in Figure 8 include *m/z* 194.0920 (14 ppm error), *m/z* 166.0993 (30 ppm error), *m/z* 164.0822 (21 ppm error), *m/z* 149.0262 (16 ppm error), 136.0866 (17 ppm error) 108.0929 (37 ppm error), and *m/z* 89.1169 (19 ppm error).

The product ion at *m/z* 194.0920 is formed through cleavage of the *N*-alkyl group, which is common for 3° amine, *N*-alkylated synthetic cathinones.[57] The product ion at *m/z* 164.0822 results from the cleavage of formaldehyde ($CH_2O$) from the intermediate at *m/z* 194.0920, and the product ion at *m/z* 149.0262 is the methylenedioxy-substituted benzoylium ion. The loss of formaldehyde from methylenedioxy-substituted cathinones has been reported previously for both *N*-alkylated synthetic cathinones and α-pyrrolidinophenone synthetic cathinones.[4,72]

Based on the $MS^n$ data from the LIT, the intermediates at *m/z* 164.0822 and *m/z* 166.0944 can continue to lose small neutrals to form product ions at *m/z* 136.0842 and *m/z* 108.0929, which are much more prominent in the higher energy beam-type CID spectrum and in-source CID than the lower energy beam-type CID spectrum.

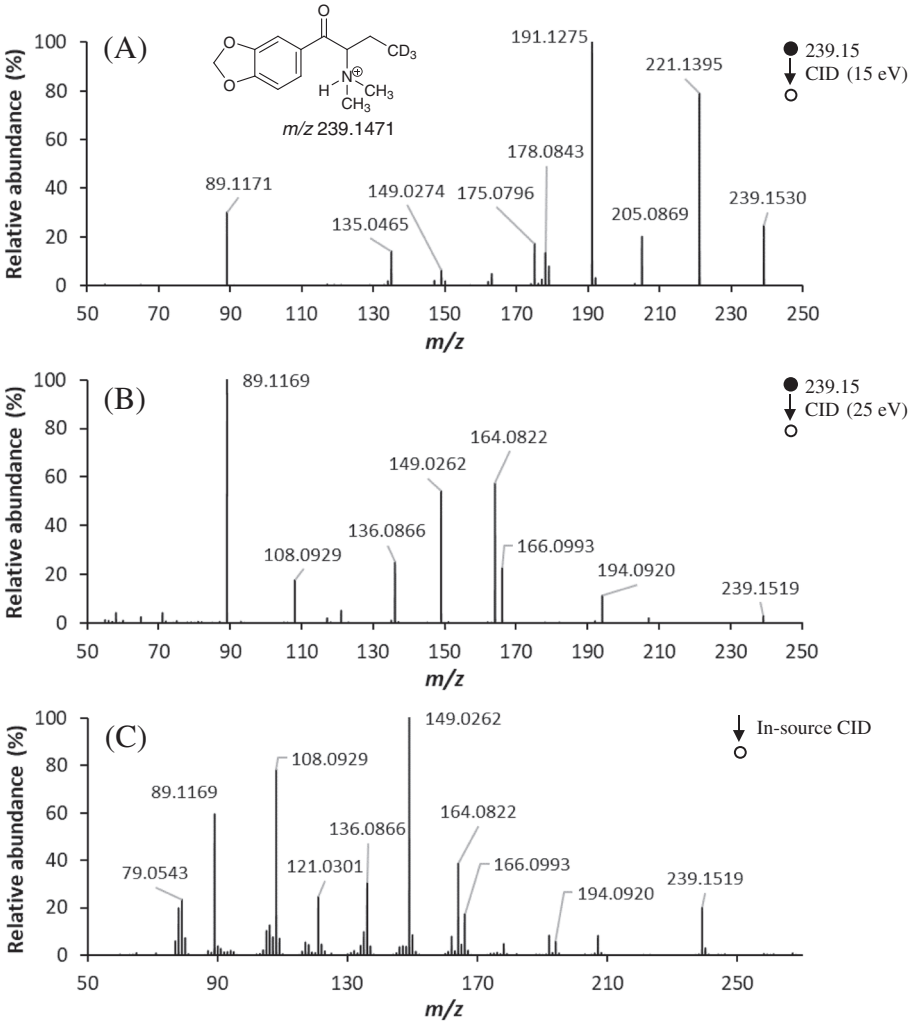


**FIGURE 8** Comparison of beam-type (CID) (top and middle) and in-source CID (bottom) for protonated dibutylone-$d_3$. For all spectra, the skimmer setting was held at 65 V. For beam-type CID, the fragmentor setting was 225 V with collision energies of 15 and 25 eV, for (A) and (B), respectively. For in-source CID, the fragmentor setting was 285 V with a collision energy of 0 eV

The authors are not aware of any mechanisms to form these lower mass fragments via direct cleavages, so their presence can only be explained by sequential neutral losses. The presence of the low-energy product ion at *m/z* 89.1169, which corresponds to the deuterated iminium ion, provides further support for the presence of a synthetic cathinone. However, this low energy product ion is less abundant in the in-source CID spectrum (Figure 8C) than the higher-energy beam-type CID spectrum (Figure 8B) because other pathways and sequential neutral losses become more competitive under in-source CID conditions. The in-source CID spectrum in Figure 8C contains greater differences in product ion abundances relative to the beam-type CID spectra at a collision energy of 15 eV in Figure 8A and at 25 eV in Figure 8B than the other spectral comparisons. Still, from the perspective of drug identification, the most abundant product ions in the beam-type CID spectra are among the most abundant product ions of the in-source CID spectra.

### 3.2.1 | Discussion for cathinone analogs

Through the analysis of a series of *N*-alkylated synthetic cathinones, we have identified the general consistency between product ion spectra of in-source CID and beam-type CID on the same instrument with the same ion source. The compounds analyzed had a range of molecular weights and various degrees of substitution, including the presence of 2° and 3° amines, which are known to favor different pathways during tandem mass spectrometry.[57] Whereas in-source CID and beam-type CID spectra are generally similar in the distribution and types of product ions formed, the spectra can be distinguished based on subtle differences in relative ion abundances and by the fact that the in-source CID spectra typically provide increased noise and additional adducts relative to beam-type CID spectra. Differences between in-source CID spectra and beam-type CID spectra can be ascribed to four major factors: (1) in-source CID spectra can include ions from different precursor molecules; (2) in-source CID spectra can contain product ions from different adducts of the same precursor molecules; (3) in-source CID spectra appear to access kinetically favored, higher-energy fragmentation pathways; and (4) in-source CID spectra seem to suffer from discrimination against low-mass product ions in the region *m/z* 50–77.

As examples of factors 1 and 2 above, the high energy in-source CID spectrum of methcathinone-$d_3$ (255 V, Figure 5C) shows an abundant product ion (peak drop-in) at *m/z* 98.9781, which is absent from the lower energy in-source CID spectrum (175 V, Figure 5B) and the beam-type CID spectrum (Figure 5A). We assume that this fragment derives from a sulfuric acid impurity or from a precursor with a higher activation energy than methcathinone-$d_3$. Supporting this hypothesis, the same product ion at *m/z* 98.9781 was observed in other in-source CID spectra, such as *ortho*-methylfentanyl (Figure 1B). The impurity could derive from a contaminant within the solvent, the residual gases, the sample container, or the ionization source itself (i.e., PEEK tubing). An example of peak drop-out for the in-source CID spectra is the product ion at *m/z* 79.0556 for $C_6H_7^+$ (expected at *m/z* 79.0547; 11 ppm error) in Figure 5A. This product ion is only present in the beam-type CID. The occurrence of ion drop-in/drop-out is particularly tricky when dealing with more complex samples or matrices than the drug standards used in this study.

The nature of in-source CID implies that the product ions generated through in-source CID arise not only from the analyte of interest but also from any compound present in the source during the in-source CID process. Practically, this means that the product ions present in the in-source CID product ion spectra are not exclusively derived from the analyte of interest. This fundamental principle limits the applicability of in-source CID for the structural elucidation of unknown compounds; however, in-source CID has demonstrated moderate success with the differentiation of structurally similar compounds such as synthetic cathinones,[25,45] synthetic cannabinoids[49] and fentanyl analogs.[26] One approach to determine which product ions in an in-source CID spectrum derive from which precursor ions in a mixture is to use chemometrics.[74] In the absence of more-extensive validation, isolation and fragmentation will continue to be required for potential unequivocal differentiation of isomers and isobars.[75]

Two approaches that have been applied in an attempt to overcome the downfalls of in-source CID are the combination of chromatography and the generation of instrument specific in-source CID mass spectral libraries.[7] Chromatography allows for the separation of the analyte of interest from other potential interferences; however, chromatography does not address source-specific contamination and coelution. The application of in-source CID mass spectral libraries can be manufacturer specific—to account for the effects of source design—and, to have the highest power of discrimination, instrument specific.[32] When feasible, the generation of composite mass spectra through summed or averaged mass spectra collected at different potentials has shown the capability to identify unknown compounds based on in-house generated in-source CID mass spectral libraries.[7]

## 4 | CONCLUSIONS

The analysis of a series of previously characterized fentanyl analogs[56] and synthetic cathinones[57] with a Q-TOF mass spectrometer allowed for a qualitative assessment of the similarities and differences in the product ion spectra generated with in-source CID and beam-type CID conditions. In this study, we demonstrate that, under certain conditions, it is possible to generate similar product ion spectra between in-source CID and beam-type CID of the same substance. However, although in-source CID and beam-type CID both encourage consecutive neutral losses at elevated collision energies, both techniques tend to produce kinetically favored fragments at lower masses relative to trapping-type CID. Of the three techniques, in-source CID seems to access the highest energy pathways and tends to show the greatest extent of peak drop-in/drop-out and elevated noise from contaminant ions. The subtle differences in relative ion abundances between in-source CID and beam-type CID can usually be explained by the preference for higher energy pathways with in-source CID, especially at

elevated fragmentor voltages. In some cases, the abundance of peaks that are separated by only a few Daltons, such as nominal *m/z* 165 and nominal *m/z* 170 for alfentanil, can show ratios as disparate as 0.75:1 for trapping-type CID to 1.25:1 for beam-type CID and ~5:1 for in-source CID.

## ACKNOWLEDGEMENTS

This project was supported by grant number 2018-75-CX-0033, awarded by the National Institute of Justice, Office of Justice Programs, and U.S. Department of Justice. The opinions, findings, and conclusions or recommendations expressed in this publication are those of the authors and do not necessarily reflect the views of the Department of Justice.

## ORCID

*J. Tyler Davidson* https://orcid.org/0000-0001-9932-8273
*Zachary J. Sasiene* https://orcid.org/0000-0001-6020-3828
*Glen P. Jackson* https://orcid.org/0000-0003-0803-6254

## REFERENCES

1. McLafferty FW, Stauffer DA, Loh SY, Wesdemiotis C. Unknown identification using reference mass spectra. Quality evaluation of databases. *J am Soc Mass Spectrom*. 1999;10(12):1229-1240.
2. Koppel C, Tenczer J. Scope and limitations of a general unknown screening by gas chromatography–mass spectrometry in acute poisoning. *J am Soc Mass Spectrom*. 1995;6(11):995-1003.
3. Weinmann W, Wiedemann A, Eppinger B, Renz M, Svoboda M. Screening for drugs in serum by electrospray ionization/collision-induced dissociation and library searching. *J am Soc Mass Spectrom*. 1999;10(10):1028-1037.
4. Zuba D. Identification of cathinones and other active components of 'legal highs' by mass spectrometric methods. *Trends Anal Chem*. 2012;32:15-30.
5. Ohta H, Suzuki S, Ogasawara K. Studies on fentanyl and related compounds IV. Chromatographic and spectrometric discrimination of fentanyl and its derivatives. *J Anal Toxicol*. 1999;23(4):280-285.
6. Sleno L, Volmer DA. Ion activation methods for tandem mass spectrometry. *J Mass Spectrom*. 2004;39(10):1091-1112.
7. Josephs JL. Characterization of over-the-counter cough/cold medications by liquid chromatography/electrospray mass spectrometry. *Rapid Commun Mass Spectrom*. 1995;9:1270-1274.
8. McLuckey SA, Goeringer DE. Slow heating methods in tandem mass spectrometry. *Int J Mass Spectrom*. 1997;32:461-474.
9. Mitchell Wells J, McLuckey SA. Collision-induced dissociation (CID) of peptides and proteins. *Methods Enzymol*, Ed. A.L. Burleingame, Editor. 2005;148-185.
10. Buré C, Lange C. Comparison of dissociation of ions in an electrospray source, or a collision cell in tandem mass spectrometry. *Curr Org Chem*. 2003;7:1613-1624.
11. Katta V, Chowdhury SK, Chait BT. Use of a single-quadrupole mass spectrometer for collision-induced dissociation studies of multiply charged peptide ions produced by electrospray ionization. *Anal Chem*. 1991;63(2):174-178.
12. Purvine S, Eppel JT, Yi EC, Goodlett DR. Shotgun collision-induced dissociation of peptides using a time of flight mass analyzer. *Proteomics*. 2003;3(6):847-850.
13. Harrison AG. Characterization of alpha- and gamma-glutamyl dipeptides by negative ion collision-induced dissociation. *J Mass Spectrom*. 2004;39(2):136-144.
14. Harrison AG. Structural and sequence effects in the fragmentation of protonated tripeptides containing tyrosine. *Can J Chem*. 2005;83(11):1969-1977.
15. Harrison AG, Young AB. Fragmentation reactions of deprotonated peptides containing aspartic acid. *Int J Mass Spectrom*. 2006;255-256:111-122.
16. Jedrzejewski PT, Lehmann WD. Detection of modified peptides in enzymatic digests by capillary liquid chromatography/electrospray mass spectrometry and a programmable skimmer CID acquisition routine. *Anal Chem*. 1997;1997(69):294-301.
17. van Berkel GJ, McLuckey SA, Glish GL. Electrospray ionization of porphyrins using a quadrupole ion trap for mass analysis. *Anal Chem*. 1991;63(11):1098-1109.
18. Crellin KC, Sibleb E, Antwerp JV. Quantification and confirmation of identity of analytes in various matrices with in-source collision-induced dissociation on a single quadrupole mass spectrometer. *Int J Mass Spectrom*. 2003;222:281-311.
19. Loo JA, Udseth HR, Smith RD. Collisional effects on the charge distribution of ions from large molecules, formed by electrospray-ionization mass spectrometry. *Rapid Commun Mass Spectrom*. 1988;2(10):207-210.
20. Smith RD, Loo JA, Barinaga CJ, Edmonds CG, Udseth HR. Collisional activation and collision-activated dissociation of large multiply charged polypeptides and proteins produced by electrospray ionization. *J am Soc Mass Spectrom*. 1990;53-65.
21. Dongen WDV, Wijk JITV, Green BN, Heerma W, Haverkamp J. Comparison between collision induced dissociation of electrosprayed protonated peptides in the up-front source region and in a low-energy. *Collision Cell*. 1999;13:1712-1716.
22. Huddleston MJ, Mark F, Bean SAC. Collisional fragmentation of glycopeptides by electrospray ionization LC/MS and LC/MS/MS: methods for selective detection of glycopeptides in protein digests. *Anal Chem*. 1993;65(7):877-884.
23. Lee SH, Choi DW. Comparison between source-induced dissociation and collision-induced dissociation of ampicillin, chloramphenicol, ciprofloxacin, and oxytetracycline via mass spectrometry. *Toxicol Res*. 2013;29(2):107-114.
24. Steiner RR, Larson RL. Validation of the direct analysis in real time source for use in forensic drug screening. *J Forensic Sci*. 2009;54(3):617-622.
25. Lesiak AD, Musah RA, Cody RB, Domin MA, Dane AJ, Shepard JR. Direct analysis in real time mass spectrometry (DART-MS) of "bath salt" cathinone drug mixtures. *Analyst*. 2013;138(12):3424-3432.
26. Sisco E, Verkouteren J, Staymates J, Lawrence J. Rapid detection of fentanyl, fentanyl analogues, and opioids for on-site or laboratory based drug seizure screening using thermal desorption DART-MS and ion mobility spectrometry. *Forens Chem*. 2017;4:108-115.
27. Bogusz MJ, Maier R-D, Kruger KD, Webb KS, Romeril J, Miller ML. Poor reproducibility of in-source collisional atmospheric pressure ionization mass spectra of toxicologically relevant drugs. *J Chromatogr a*. 1999;844(1-2):409-418.
28. Forbes TP, Sisco E. In-source collision induced dissociation of inorganic explosives for mass spectrometric signature detection and chemical imaging. *Anal Chim Acta*. 2015;892:1-9.
29. Lips AGAM, Lameijer W, Fokkens RH, Nibbering NMM. Methodology for the development of a drug library based upon collision-induced fragmentation for the identification of toxicologically relevant drugs in plasma samples. *J Chromatogr B*. 2001;739:191-207.
30. Harrison AG. Energy-resolved mass spectrometry: a comparison of quadrupole cell and cone-voltage collision-induced dissociation. *Rapid Commun Mass Spectrom*. 1999;13(16):1663-1670.
31. Parcher JF, Wang M, Chittiboyina AG, Khan IA. In-source collision-induced dissociation (IS-CID): applications, issues and structure elucidation with single-stage mass analyzers. *Drug Test Anal*. 2018;10(1):28-36.

32. Bristow AW, Nichols WF, Webb KS, Conway B. Evaluation of protocols for reproducible electrospray in-source collisionally induced dissociation on various liquid chromatography/mass spectrometry instruments and the development of spectral libraries. *Rapid Commun Mass Spectrom*. 2002;16(24):2374-2386.
33. Collette C, Drahos L, Pauw ED, Ve'key K. Comparison of the internal energy distributions of ions produced by different electrospray sources. *Rapid Commun Mass Spectrom*. 1998;12:1673-1678.
34. Gabelica V, De Pauw E. Internal energy and fragmentation of ions produced in electrospray sources. *Mass Spectrom Rev*. 2005;24(4):566-587.
35. Collette C, Pauw ED. Calibration of the internal energy distribution of ions produced by electrospray. *Rapid Commun Mass Spectrom*. 1998;12:165-170.
36. Schneider BB, Douglas DJ, Chen DDY. Ion fragmentation in an electrospray ionization mass spectrometer interface with different gases. *Rapid Commun Mass Spectrom*. 2001;15(4):249-257.
37. Weinmann W, Stoertzel M, Vogt S, Svoboda M, Schreiber A. Tuning compounds for electrospray ionization/in-source collision-induced dissociation and mass spectra library searching. *J Mass Spectrom*. 2001;36(9):1013-1023.
38. Weinmann W, Stoertzel M, Vogt S, Wendt J. Tune compounds for electrospray ionisation /in-source collision-induced dissociation with mass spectral library searching. *J Chromatogr a*. 2001;926:199-209.
39. Marquet P, Venisse N, Lacassie É, Lachâtre G. In-source CID mass spectral libraries for the "general unknown" screening of drugs and toxicants. *Analusis*. 2000;28(10):925-934.
40. Qi LW, Cao J, Li P, et al. Qualitative and quantitative analysis of Radix Astragali products by fast high-performance liquid chromatography-diode array detection coupled with time-of-flight mass spectrometry through dynamic adjustment of fragmentor voltage. *J Chromatogr a*. 2008;1203(1):27-35.
41. Gwak S, Almirall JR. Rapid screening of 35 new psychoactive substances by ion mobility spectrometry (IMS) and direct analysis in real time (DART) coupled to quadrupole time-of-flight mass spectrometry (QTOF-MS). *Drug Test Anal*. 2015;7(10):884-893.
42. Pavlovich MJ, Musselman B, Hall AB. Direct analysis in real time-mass spectrometry (DART-MS) in forensic and security applications. *Mass Spectrom Rev*. 2018;37(2):171-187.
43. Cody RB, Laremée JA, Durst HD. Versatile new ion source for the analysis of materials in open air under ambient conditions. *Anal Chem*. 2005;77(8):2297-2302.
44. Gross JH. Direct analysis in real time—a critical review on DART-MS. *Anal Bioanal Chem*. 2014;406(1):63-80.
45. Power JD, McDermott SD, Talbot B, O'Brien JE, Kavanagh P. The analysis of amphetamine-like cathinone derivatives using positive electrospray ionization with in-source collision-induced dissociation. *Rapid Commun Mass Spectrom*. 2012;26(22):2601-2611.
46. Musah RA, Cody RB, Domin MA, Lesiak AD, Dane AJ, Shepard JR. DART-MS in-source collision induced dissociation and high mass accuracy for new psychoactive substance determinations. *Forensic Sci Int*. 2014;244:42-49.
47. Fowble KL, Shepard JRE, Musah RA. Identification and classification of cathinone unknowns by statistical analysis processing of direct analysis in real time-high resolution mass spectrometry-derived "neutral loss" spectra. *Talanta*. 2018;179:546-553.
48. Sisco E, Forbes TP, Staymates ME, Gillen G. Rapid analysis of trace drugs and metabolites using a thermal desorption DART-MS configuration. *Anal Methods*. 2016;8(35):6494-6499.
49. Musah RA, Domin MA, Cody RB, Lesiak AD, Dane AJ, Shepard JR. Direct analysis in real time mass spectrometry with collision-induced dissociation for structural analysis of synthetic cannabinoids. *Rapid Commun Mass Spectrom*. 2012;26(19):2335-2342.
50. Lesiak AD, Adams KJ, Domin MA, Henck C, Shepard JR. DART-MS for rapid, preliminary screening of urine for DMAA. *Drug Test Anal*. 2014;6:7-8. 788-796
51. Lesiak AD, Cody RB, Ubukata M, Musah RA. Direct analysis in real time high resolution mass spectrometry as a tool for rapid characterization of mind-altering plant materials and revelation of supplement adulteration—the case of Kanna. *Forensic Sci Int*. 2016;260:66-73.
52. Lesiak AD, Musah RA. Application of ambient ionization high resolution mass spectrometry to determination of the botanical provenance of the constituents of psychoactive drug mixtures. *Forensic Sci Int*. 2016;266:271-280.
53. Abranko L, Garcia-Reyes JF, Molina-Diaz A. In-source fragmentation and accurate mass analysis of multiclass flavonoid conjugates by electrospray ionization time-of-flight mass spectrometry. *J Mass Spectrom*. 2011;46(5):478-488.
54. Perez-Ortega P, Lara-Ortega FJ, Garcia-Reyes JF, Gilbert-Lopez B, Trojanowicz M, Molina-Diaz A. A feasibility study of UHPLC-HRMS accurate-mass screening methods for multiclass testing of organic contaminants in food. *Talanta*. 2016;160:704-712.
55. Fornal E. Study of collision-induced dissociation of electrospray-generated protonated cathinones. *Drug Test Anal*. 2014;6(7-8):705-715.
56. Davidson JT, Sasiene ZJ, Jackson GP. The influence of chemical modifications on the fragmentation behavior of fentanyl and fentanyl-related compounds in electrospray ionization tandem mass spectrometry. *Drug Test Anal*. 2020;12(7):957-967.
57. Davidson JT, Sasiene ZJ, Jackson GP. Fragmentation pathways of odd- and even-electron *N*-alkylated synthetic cathinones. *Int J Mass Spectrom*. 2020;453:116354. https://doi.org/10.1016/j.ijms.2020.116354
58. Wichitnithad W, McManus TJ, Callery PS. Identification of isobaric product ions in electrospray ionization mass spectra of fentanyl using multistage mass spectrometry and deuterium labeling. *Rapid Commun Mass Spectrom*. 2010;24(17):2547-2553.
59. Davidson JT, Sasiene ZJ, Jackson GP. The characterization of isobaric product ions of fentanyl using multi-stage mass spectrometry, high-resolution mass spectrometry and isotopic labeling. *Drug Test Anal*. 2020;12(4):496-503.
60. Olah GA, Spear RJ, Forsyth DA. Rearrangement of ethylenebenzenium ions to a-phenylethyl (styryl) cations. Determination of the relative energies of the a-bridged ethylenebenzenium ion, the open-chain 2-phenylethyl cation, and the a-styryl cation. *J Am Chem Soc*. 1976;98(20):6284-6289.
61. Thevis M, Geyer H, Bahr D, Schanzer W. Identification of fentanyl, alfentanil, sufentanil, remifentanil and their major metabolites in human urine by liquid chromatography/tandem mass spectrometry for doping control purposes. *Eur J Mass Spectrom*. 2005;11(4):419-427.
62. Grzeskowiak T, Zgola-Grzeskowiak A, Rusinska-Roszak D, Zaporowska-Stachowiak I, Jeszka-Skowron M. Fragmentation studies of selected drugs utilized in palliative care. *Eur J Mass Spectrom*. 2018;420-436.
63. Palmquist KB, Swortwood M. Quantification of Furanyl fentanyl and its metabolites in human and rat plasma using LC-MS/MS. *J Anal Toxicol*. 2020;44(6):589-595.
64. Nan Q, Hejian W, Ping X, et al. Investigation of fragmentation pathways of fentanyl analogues and novel synthetic opioids by electron ionization high-resolution mass spectrometry and electrospray ionization high-resolution tandem mass spectrometry. *J Am Soc Mass Spectrom*. 2020;31(2):277-291.
65. Muller C, Vogt S, Goerke R, Kordon A, Weinmann W. Identification of selected psychopharmaceuticals and their metabolites in hair by LC-ESI-CID-MS and MS-MS. *Foresic Sci Int*. 2000;113:415-421.
66. Fornal E. Formation of odd-electron product ions in collision-induced fragmentation of electrospray-generated protonated cathinone

derivatives: aryl alpha-primary amino ketones. *Rapid Commun Mass Spectrom*. 2013;27(16):1858-1866.
67. Majchrzak M, Celinski R, Kowalska T, Sajewicz M. Fatal case of poisoning with a new cathinone derivative: alpha-propylaminopentiophenone (N-PP). *Forensic Toxicol*. 2018;36(2):525-533.
68. Jankovics P, Varadi A, Tolgyesi L, Lohner S, Nemeth-Palotas J, Koszegi-Szalai H. Identification and characterization of the new designer drug 4′-methylethcathinone (4-MEC) and elaboration of a novel liquid chromatography-tandem mass spectrometry (LC-MS/MS) screening method for seven different methcathinone analogs. *Forensic Sci Int*. 2011;210(1-3):213-220.
69. Pozo OJ, Ibanez M, Sancho JV, et al. Mass spectrometric evaluation of mephedrone in vivo human metabolism: identification of phase I and phase II metabolites, including a novel succinyl conjugate. *Drug Metab Dispos*. 2015;43(2):248-257.
70. Bijlsma L, Sancho JV, Hernandez F, Niessen WM. Fragmentation pathways of drugs of abuse and their metabolites based on QTOF MS/MS and $MS^E$ accurate-mass spectra. *J Mass Spectrom*. 2011;46(9):865-875.
71. Zancanaro I, Limberger RP, Bohel PO, et al. Prescription and illicit psychoactive drugs in oral fluid—LC-MS/MS method development and analysis of samples from Brazilian drivers. *Forensic Sci Int*. 2012;223(1–3):208-216.
72. Davidson JT, Sasiene ZJ, Abiedalla Y, DeRuiter J, Clark CR, Jackson GP. Fragmentation pathways of α-pyrrolidinophenone synthetic cathinones and their application to the identification of emerging synthetic cathinone derivatives. *Int J Mass Spectrom*. 2020;453:116343. https://doi.org/10.1016/j.ijms.2020.116343
73. Davidson JT, Piacentino EL, Sasiene ZJ, et al. Identification of novel fragmentation pathways and fragment ion structures in the tandem mass spectra of protonated synthetic cathinones. *Forens Chem*. 2020;19:100245. https://doi.org/10.1016/j.forc.2020.100245
74. Grange AH, Sovocool GW. Automated determination of precursor ion, product ion, and neutral loss compositions and deconvolution of composite mass spectra using ion correlation based on exact masses and relative isotopic abundances. *Rapid Commun Mass Spectrom*. 2008;22(15):2375-2390.
75. Brown H, Oktem B, Windom A, Doroshenko V, Evans-Nguyen K. Direct analysis in real time (DART) and a portable mass spectrometer for rapid identification of common and designer drugs on-site. *Forens Chem*. 2016;1:66-73.

## SUPPORTING INFORMATION

Additional supporting information may be found online in the Supporting Information section at the end of this article.

**How to cite this article:** Davidson JT, Sasiene ZJ, Jackson GP. Comparison of in-source collision-induced dissociation and beam-type collision-induced dissociation of emerging synthetic drugs using a high-resolution quadrupole time-of-flight mass spectrometer. *J Mass Spectrom*. 2020;56:e4679. https://doi.org/10.1002/jms.4679